PNC-TN9410 88-048

Presented at the 9th annual
conference of the Canadian
Nuclear Society, Winnipeg, Manitoba, Canada
June 12-15, 1988.

REFLOODING PHENOMENA DURING ECCS OPERATION

MAY, 1988

OARAI ENGINEERING CENTER
POWER REACTOR AND NUCLEAR FUEL DEVELOPMENT CORPORATION

複製又はこの資料の入手については，下記にお問い合わせください。
〒311-13　茨城県東茨城郡大洗町成田町4002
動力炉・核燃料開発事業団
大洗工学センター　システム開発推進部・技術管理室

Enquires about copyright and reproduction should be addressed to: Technology Management Section O-arai Engineering Center, Power Reactor and Nuclear Fuel Development Corporation 4002 Narita-cho, O-arai-machi, Higashi-Ibaraki, Ibaraki-ken, 311-13, Japan

動力炉・核燃料開発事業団（Power Reactor and Nuclear Fuel Development Corporation）

PNC-TN9410 88-048
MAY, 1988

REFLOODING PHENOMENA DURING ECCS OPERATION

H. MOCHIZUKI AND Y. HAYAMIZU

O-arai Engineering Center
Power Reactor and Nuclear Fuel Development Corporation (PNC)
4002, Narita, O-arai, Ibaraki 311-13, Japan

ABSTRACT

Turn-around time, heat transfer coefficient after turn-around, and quench temperature were measured and correlated for various kinds of heater bundles and ECC water conditions. Applicability of the quench temperature correlation to the safety analysis has been verified by the analysis of the system tests using the full mock-up safety facility of the ATR.

INTRODUCTION

The emergency core cooling system (ECCS) of the Advanced Thermal Reactor (ATR) consists of three types of systems, i.e. a High Pressure Core Injection (HPCI) system, a Low Pressure Core Injection (LPCI) system, and an Accumulated Pressurized Core Injection (APCI) system. The role of HPCI is to decrease the system pressure by spraying water into a steam region in a steam drum when a small break occurs and the system pressure hardly decreases. When the system pressure decreases to around 4MPa, the APCI system is alwaysinitiated and thereafter the APCI system is succeeded by LPCI.

Because the core of the ATR is vertical, there are two possible reflooding modes after injection of ECC water in the case of loss of coolant accidents (LOCAs). When a pipe rupture occurs, the coolant of APCI is injected into a water drum which is a header of feeder pipes. In the case of a downcomer, a main steam pipe, or a riser tube breaks, bottom flooding occurs. On the other hand, when a feeder pipe breakes, top flooding is taken place by water from the steam drum. Moreover, the ATR has a characteristic that the reflooding speed of bottom flooding is quite high compared with that of light water reactors (LWRs). It is because a fuel bundle is provided in a pressure tube with a concentric arrangement, and flow area is rather narrow. PNC has conducted reflooding tests which consist of characteristic tests and system tests using the ATR safety experimental facility. Hayamizu [1] studied the thermocouple instrumentation methods for measurement of heater rod surface temperature during reflooding. As a result, several instrumentation method were developed.

BOTTOM FLOODING EXPERIMENT

Apparatus and Experimental Conditions

The schematic flow diagram of the apparatus is illustrated in Fig. 1. Cooling water was pressureized to 1 MPa in an accumulator by nitrogen gas and injected into the test section through a quick opening pneumatic valve, a turbine flow meter, and a flow control valve. Tests were conducted using single channel or parallel channels in which 28-rod or 36-rod bundle heaters were housed. Not only

normal shaped heater bundles but also a bundle simulating a ballooning assembly shown in Fig. 2 was used to study the difference in cooling characteristics. To simulate the ballooning heater, blockages of 0.222 m in length were mounted on heater rods. Figure 3 illustrates an example of the thermocouple arrangement on the 36-rod heater. Table 1 & 2 show the size of the channel and heat fluxes of the heater in several locations, respectively.

A downcomer break port illustrated in Fig.1 was used to conduct system tests including blowdown and ECCS operation.

The following test conditions were chosen to cover the operational condition of the real reactor.

1) flooding velocity: 0.02 to 1.27 m/s
2) pressure: atmospheric, 0.4-6.3 MPa
3) initial cladding temperature: 350 to 850 ℃
4) coolant temperature: around 30℃
5) power distribution: chopped cosine
6) linear heat rate: 1.02 to 1.95 kW/m

Results

There are three typical characteristics related to reflooding. They are turnaround, heat transfer after turn-around of cladding temperature, and quenching.

Heat transfer in the reflooding process depends on the configuration of the fuel cluster as well as thermal hydraulic conditions. Turn-around starts from both sides, i.e. bottom and top, of the cluster in the ATR's fuel. It has been clarified that turn-around time at a given elevation is correlated as a function of reflooding volocity as shown in Fig.4. Turn-around time defined as the time required for the slope of the cladding temperature rise to reach zero after ECC water arrives at the inlet of the heated section is correlated by the following dimensionless expression.

$$\frac{t \cdot V}{x} = 11 \left(\frac{x}{x_H} - 0.6 \right)^4 + 0.12 \qquad (1)$$

t(s) is turn-around time, V(m/s) reflooding velocity, x(m) elevation from the bottom of the heated section, and x_H (m) effected heated lengt. Figure 5 shows the comparison between experimental data for both normal and ballooning clusters and the correlation. Data scatter around the correlation within the error of 20-30%.

Heat transfer coefficients after turn-around were calculated from rod surface temperatures using the one-dimension-al heat conduction code "OLION". The heat transfer coefficient after turn-around is nearly constant as shown in Fig.6. Time-averaged heat transfer coefficients are correlated as a function of time-averaged reflooding velocity for both normal and ballooned clusters. The average velocity is used because the reflooding velocity after turn-around oscillates. The heat transfer coefficients at the middle part of the heater are lowest in the cluster, as shown in Fig. 7, and are correlated as follows.

$$Nu = 0.0304\ Re^{0.5}\ Pr^{0.4} \qquad (2)$$

where the Reynolds number and the Prandtl number are defined using physical properties in the saturated condition. The heat transfer coefficient of film boiling increases as the 0.8th power of the Reynolds number under forced

convection flow regime. However, gradient of the film boiling heat transfer coefficient against flow rate in bottom flooding is more gentle.

Generally, there are two methods to express quenching. One is an expression using the quench fromt velocity. In this case, it is usually treated that a quench front moves from bottom to top. The other expression is to correlate the quench temperature as a function of several factors such as physical properties and testing conditions. In our experiment, it was observed that quench fronts moved from the bottom and top to the middle and met each other at the position between the top and the center as shown in Fig.8. Therefore, a model that the quench front moves from the bottom to the top can not appropriately express quenching which occurs in the ATR.

Effecting factors on quenching by fuel rods are heat flux, peak cladding temperature, heat capacity, thermal conductivity, and surface conditions, and coolant conditions, i.e.pressure, subcooling, and velocity. Heat capacity and thermal conductivity of the heater rods simulate UO_2 pellets and the cladding of a real fuel pin, as shown in Table 3. Heater surface conditions have an effect on quenching from the stand point of wetness. However, its effect would be small. Subcooling may also have an effect on quenching. However, coolant reaches the saturation condition soon after coolant goes up. After all, heat flux, peak cladding temperrature, pressure, and reflooding velocity were chosen as effecting parameters on quenching in the study. Siegel-Carbajo[2] correlated the quench temperature as a function of these four parameters. But this correlation did not predict well quench temperatures obtained in our experiment. It is probably because they made their correlation based on the PWR-FLECHT[3] test in which reflooding velocity was in the range of 0.003-0.03 m/s. It is quite slow compared with reflooding velocity of the ATR.

Figure 9 shows the relationship between quench temperature ΔT_Q ($=T_Q - T_S$) and average reflooding velocity. Quench temperature increases with reflooding velocity in the region where velocity is greater than 0.2 m/s. On the other hand, quench temperature decreases with reflooding velocity in the region where velocity is greater than 0.02 m/s and less than 0.08 m/s. The effect of reflooding velocity on quench temperature is constant in the other regions.

Figure 10 shows the effect of peak cladding temperature T_P on quench temperature ΔT_{PT} ($=T_Q - T_S$) as a function of reflooding velocity ranging 0.08 to 0.2 m /s for various linear heat rates. The data are correlated by the following expression.

$$\Delta T_{PT} = 231.0 + 0.0752\, T_P \quad \text{for } 1.0 \leqq q \leqq 26 \text{ kW/m},\ 350 \leqq T_P \leqq 850\ ^\circ\text{C} \qquad (3)$$

The dependence of quench temperature on reflooding verocity is correlated by dividing ΔT_Q by ΔT_{PT}.

$$F_V = \frac{\Delta T_Q}{\Delta T_{PT}} = \begin{cases} 1.5 & \text{for } V \leqq 0.02 \text{ m/s} \\ 0.47V^{-0.3} & \text{for } 0.02 < V \leqq 0.08 \text{ m/s} \\ 1.0 & \text{for } 0.08 < V \leqq 0.2 \text{ m/s} \\ 1.38V^{0.2} & \text{for } 0.2 < V \leqq 1.3 \text{ m/s} \end{cases} \qquad \cdots\cdots\cdots (4)$$

As the result, quench temperatures obtained by characteristic tests are predicted by the following correlation.

$$T_Q = T_S + \Delta T_{PT} \cdot F_V \qquad \cdots\cdots\cdots (5)$$

Quench temperature also depends upon pressure. Equation (5) is applied to

blowdown data to correlate the dependence of quench temperature on pressure. Figure 11 shows the factor of pressure on quench temperature. This shows that quench temperature decreases with pressure when pressure is less than 2 MPa, and is almost constant when pressure is higher than 2 MPa.

$$F_P = \begin{cases} 0.68 - 0.32 \log_{10} P & \text{for } 0.1 \leq P \leq 2 \text{ MPa} \\ 0.584 & \text{for } 2 < P < 7 \text{ MPa} \end{cases} \quad \cdots\cdots\cdots (6)$$

In this way, the following quench correlation is obtained.

$$T_Q = T_S + \Delta T_{PT} \cdot F_V \cdot F_P \quad \cdots\cdots\cdots (7)$$

The comparison of quench temperature between measured and predicted is shown in Fig.12. Quench temperature at the hottest point can be predicted within the error of ± 10%. Most data including blowdown and bottom flooding using ballooning heater can be also predicted by the correlation within the error of ±15%.

TOP FLOODING EXPERIMENT

Apparatus and experimental conditions

The same apparatus shown in Fig. 1 was used to conduct top flooding experiments. However, in this case a pressure tube made of glass was provided at the upper part of the test section to observe the arrival of coolant at the top of the heater. The inlet pipe connected to the test section was left open in the atmosphere to simulate the postulated double ended break of the feeder pipe. Coolant was supplied to the steam drum by an LPCI pump after initial bundle heater conditions were prepared. Experimental conditions listed below were chosen.

1) supplying water flow rate : 40 to 50 m^3/h
2) pressure : atmospheric
3) initial cladding temperature : 500 to 740 ℃
4) coolant temperature : 70 to 90 ℃

Results

It was clarified that top flooding phenomena was dominated by the countercurrent flow limiting (CCFL). When water was supplied to the test section through the riser tube which consists of horizontal part having 2 degree gradient, and vertical part as shown in Fig. 1, vapor generated in the heated section prevented water from flowing into the heated section. The CCFL occurred at orificing position where a shield plug for neutron shielding was provided. The ECC water supplied into the steam drum was 125 to 140 liters/s simulating LPCI water injection flow rate in the real reactor. However, the coolant flowing into the break channel was restricted to 1-1.7 liters/s. Therefore, almost all water supplied into the steam drum contributed to raise the water level of the steam drum.

Coolant arrival time to the core after the initiation of the reverse flow from the steam drum was dominated by the horizontal length of the riser. Because the velocity of the water front like a wedge is very slow in the horizontal region. We observed the flow regime of air-water under atmospheric condition using a lucite mock-up. Figure 13 shows the relationship between coolant arrival time to the core and turn-around time and injection flow rate. The coolant arrival

time was measured by observation through a glass tube, and turn-around time was measured by the outputs of thermocouples. This figure shows that there is a small delay between coolant arrival time and turn-around time. Moreover, this figure shows that the effect of injection flow rate on these times is exponential. Wedge shaped water front proceeding velocity V(m/s) is correlated as a function of injection flow rate Q(m^3/h) by the following expression when velocity in the vertical riser is neglected.

$$V = \frac{1}{2.48 \exp(-2.7\times10^{-2} Q) + 1.08} \quad \cdots\cdots\cdots (8)$$

Therefore, coolant arrival time to the top of the core is estimated as follows by dividing the horizontal riser length L_H by V.

$$t_1 = L_H \{2.48 \exp(-2.7 \times10^{-2} Q) + 1.08\} \quad \cdots\cdots\cdots (9)$$

Turn-around time for top flooding is vague, however it is in the order estimated by the Equation (1). In this case, however, length x(m) should be defined from the top of the heated section.

Histories of heat transfer coefficients after turn-around for top flooding are shown in Fig.14. The heat transfer coefficients are nearly constant like the bottom flooding curves shown in Fig.6 except those near the top. In the case of top flooding, estimation of flooding velocity is very difficult. However, coolant flow rate drained through the riser is estimated by the equation of Wallis [4] as about 1liter/s. Therefore, flooding velocity is roughly estimated as 0.2 m/s. The heat transfer coefficient after turn-around is about 35 W/m^2K, and is only about 20% of that of bottom flooding.

Quench temperatures of top flooding are shown in Fig.9 together with those of bottom flooding. The quench temperatures of low flow rate less than 0.01 m/s for both top and bottom floodings seemed constant. In the correlation of Siegel-Carbajo which is applied upto 0.03 m/s reflooding velocity, the power of the velocity is small as well.

DISCUSSION

In bottom flooding, it has been clarified that there are two types of quench fronts. One goes up from the bottom and the other descends from the top. The mechanism of the descending quench front seems to have connection with the structure of the fuel bundle and the power distribution. When ECC water is injected into the pressure tube, water is splashed by the high temperature claddings. Therefore vapor flow accompanies a lot of droplets. These droplets seems to be collected by the tie plate of the fuel bundle. Moreover, power level of the upper part is low because of power distribution. Therefore, cladding temperature of the upper part of the fuel are apt to turn-around. Once turn-around occurs, heat transfer coefficient increases, and heat is removed by water collected beneath the tie plate. Then, quench occurs at the top of the fuel, and this promotes collection of water beneath the tie plate.

To verify the applicability of the proposed quench correlation, comparison between the correlation and data measured by cheng et al. [5] was carried out. They measured quench temperatures for various conditions using a circular tube heater of 91.4cm in length, 1.1cm in inner diameter and 1.04mm in thickness. Figure 15 shows the comparison for the data measured at 344 kPa in pressure and for about 0.05 to 0.4 m/s in reflooding velocity. Quench temperatures are predicted to within ± 5% error.

It is important to show the applicability of the quench correlations which is used together with many thermal hydraulic models. Correlations mentioned before were incorporated into safety analysis codes to predict cladding temperatures at various positions during blowdown tests conducted using the ATR safety experimental facility. Figure 16 shows the results of bottom floodong after a 150mm downcomer break and a 150 mm main steam pipe break. In these cases, 3MW heating power was continuously supplied for about 30 or 22 seconds, respectively, and was decreased to the level of decay heat power. Cladding temperatures increased after ECC water was injected into the water drum. Because condensation of vapor generated by depressurization prevented coolant from flowing into the core. Quenching had occurred when the cladding temperature was around 400℃. General behaviors of cladding temperature are predicted by the safety analysis code SENHOR. Especially, figures show that quench temperatures at different locations and events are predicted with good accuracy.

CONCLUSIONS

Correlations in regard to turn-around time, heat transfer coefficient after turn-around, and quench temperature associated with ECC water injection have been proposed. These correlations are valid for both normal and ballooned clusters. Moreover, the quench temperature correlation can be used for not only a reflooding process but also for a rewetting due to an increase in flow rate during blowdown phase. Applicability of the quench temperature correlation to the safety analysis has been verified by the analysis of the system tests using the full mock-up safety facility of the ATR.

NOMENCLATURE

D_h : thermal equivalent diameter (m)
h : heat transfer coefficient (W/m^2K)
k : thermal conductivity (W/mK)
L_H : length of horizontal part of riser tube (m)
N_u : Nusselt number ($=h \cdot D_h / k$)
P_r : Prandtl number
Q : volumetric flow rate (m^3/h)
R_e : Reynolds number ($=V \cdot D_h / \nu_g$)
t : turn-around time (s)
T_p : peak cladding temperature (℃)
T_q : quench temperature (℃)
T_s : saturation temperature (℃)
V : average reflooding velocity (m/s)
x : location (m)
x_H : effective heated length (m)
ν_g : kinematic viscosity of saturated vapor. (m^2/s)

REFERENCES

(1) Hayamizu, Y., Kitahara, T. and Adachi, J., "Bottom Flooding Heat Transfer in a Pressure Tube Type Reactor ", Proceedings of JUICE Meeting, Toronto, Canada, (1978).

(2) Siegel, A.D. and Carbajo, J.J., "A New Experimental Correlation for the Rewetting Temperature", Trans. Am. Nucl. Soc., 35, (1980).

(3) Langerman, M.A., "Quick Look Report for Semiscale MOD-1 Test S-06-3 (LOFT Counterpart Test)", NUREG/CR-0251 (July 1978).

(4) Wallis, G.B., "One-dimensional Two-phase Flow", McGraw-Hill Book Company, (1969).

(5) Cheng, C.C., Lau, P.W.K. and Poon, K.T., "Measurements of True Quench Temperature of Subcooled Water Under Forced Convective Conditions ", Int. J. Heat Mass Transfer, 28, 1, (1985).

TABLE 1 CONFIGURATION OF TEST CHANNEL

ITEM \ TEST CHANNEL	HIGH POWER CHANNEL	LOW POWER CHANNEL
AXIAL HEAT FLUX	COSINE	UNIFORM
NUMBER OF HEATER PINS	36	28
OUTER DIAMETER OF HEATER PINS (mm)	14.5	15.9
NUMBER OF TIE ROD AND DIAMETER (mm)	1 14.5	4 9
EFFECTIVE HEATED LENGTH (mm)	3,700	3,700
INNER DIAMETER OF PRESSURE TUBE (mm)	117.8	120.8
FLOW AREA (m^2)	4.8×10^{-3}	5.65×10^{-3}
HYDRAULIC EQUIVALENT DIAMETER (m)	9.34×10^{-3}	11.95×10^{-3}
THERMAL EQUIVALENT DIAMETER (m)	11.7×10^{-3}	16.2×10^{-3}

TABLE 2 HEAT FLUX AT EACH POSITION

UNIT : (W/m^2)

AXIAL POSITION	AXIAL PEAKING	INNER PINS	MIDDLE PINS	OUTER PINS
		LOCAL PEAKING		
		0.65	1.00	1.12
I	0.63	1.3459×10^4	2.0735×10^4	2.3226×10^4
II	1.05	2.2433×10^4	3.4559×10^4	3.8710×10^4
III	1.16	2.4782×10^4	3.8180×10^4	4.2766×10^4
IV	0.8	1.7091×10^4	2.6330×10^4	2.9494×10^4

TABLE 3 THERMAL PROPERTIES OF HEATER AND PELLET

ITEM	HEATER (MgO)	BN	PELLET (UO_2)	NOTE
THEORETICAL DENSITY (kg/m^3)	3,580	2,270	10,960	
ACTUAL DENSITY (kg/m^3)	3,000	1,850	10,400	
SPECIFIC HEAT (kJ/kg K)	1.09	0.879	0.314	AT 973K
HEAT CAPACITY (kJ/m^3 K)	3,266	1,633	3,266	AT 973K
THERMAL CONDUCTIVITY (W/m K)	3.5	29.1	3.3	AT 973K
THERMAL DIFFUSIVITY (m^2/s)	1.08×10^{-6}	1.78×10^{-5}	1.0×10^{-6}	AT 973K

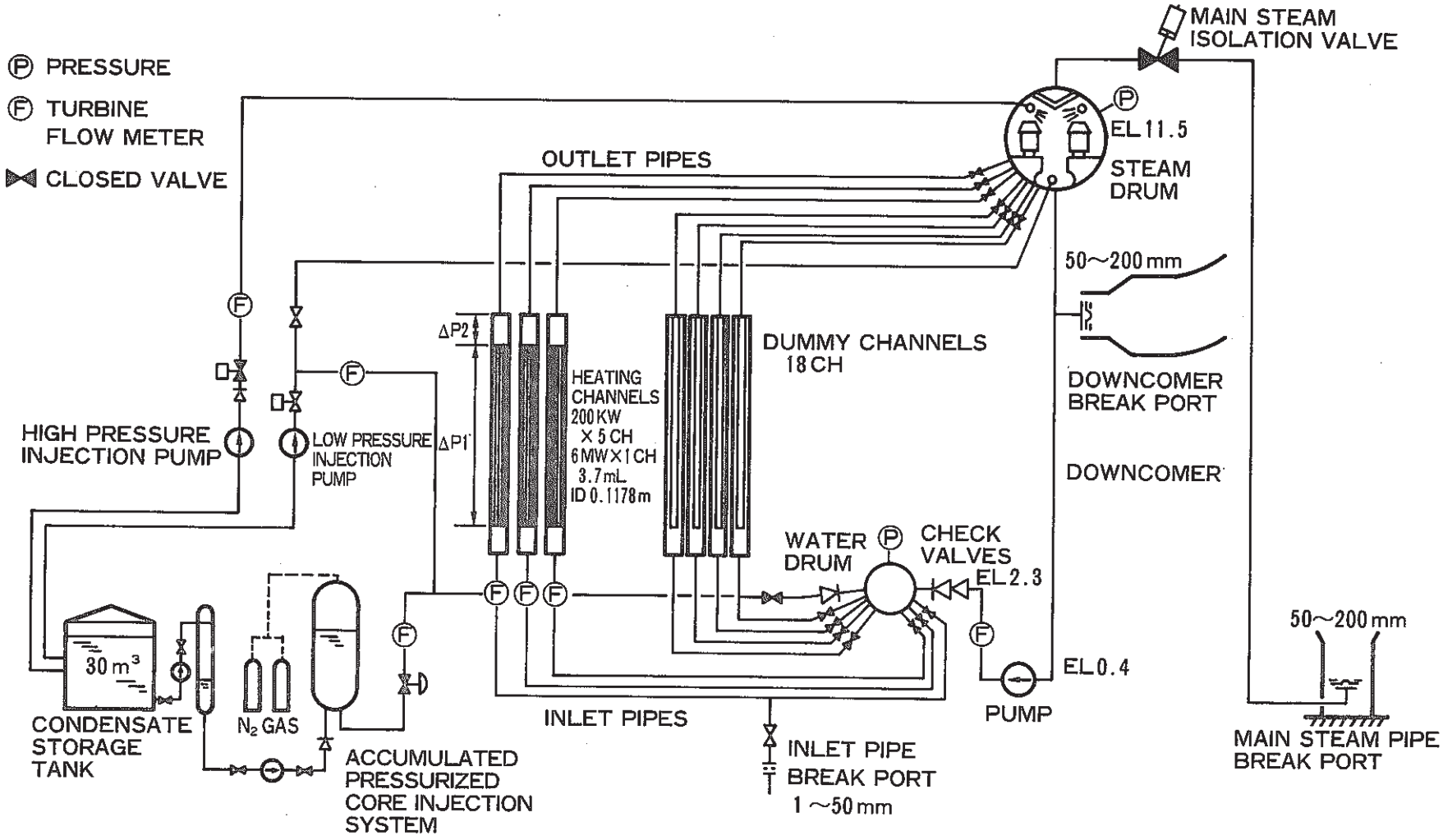

FIG. 1 ATR SAFETY EXPERIMENTAL FACILITY

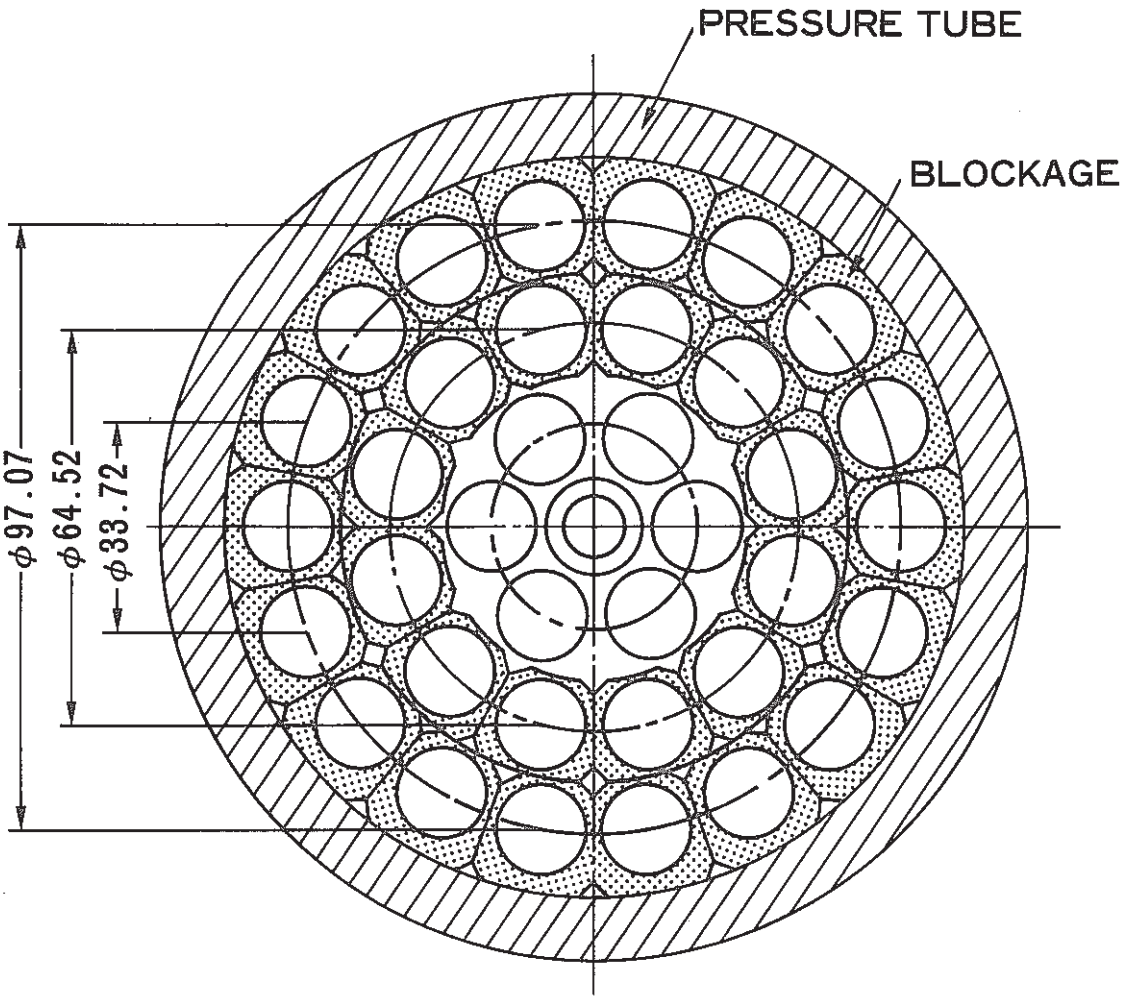

FIG. 2 CROSS SECTIONAL VIEW OF BLOCKAGE HEATER

TOTAL POWER 200KW
- OUTER 6.2 KW/PIN×18=112KW
- MIDDLE 5.55 KW/PIN× 2= 67KW
- INNER 3.6 KW/PIN× 6= 21KW

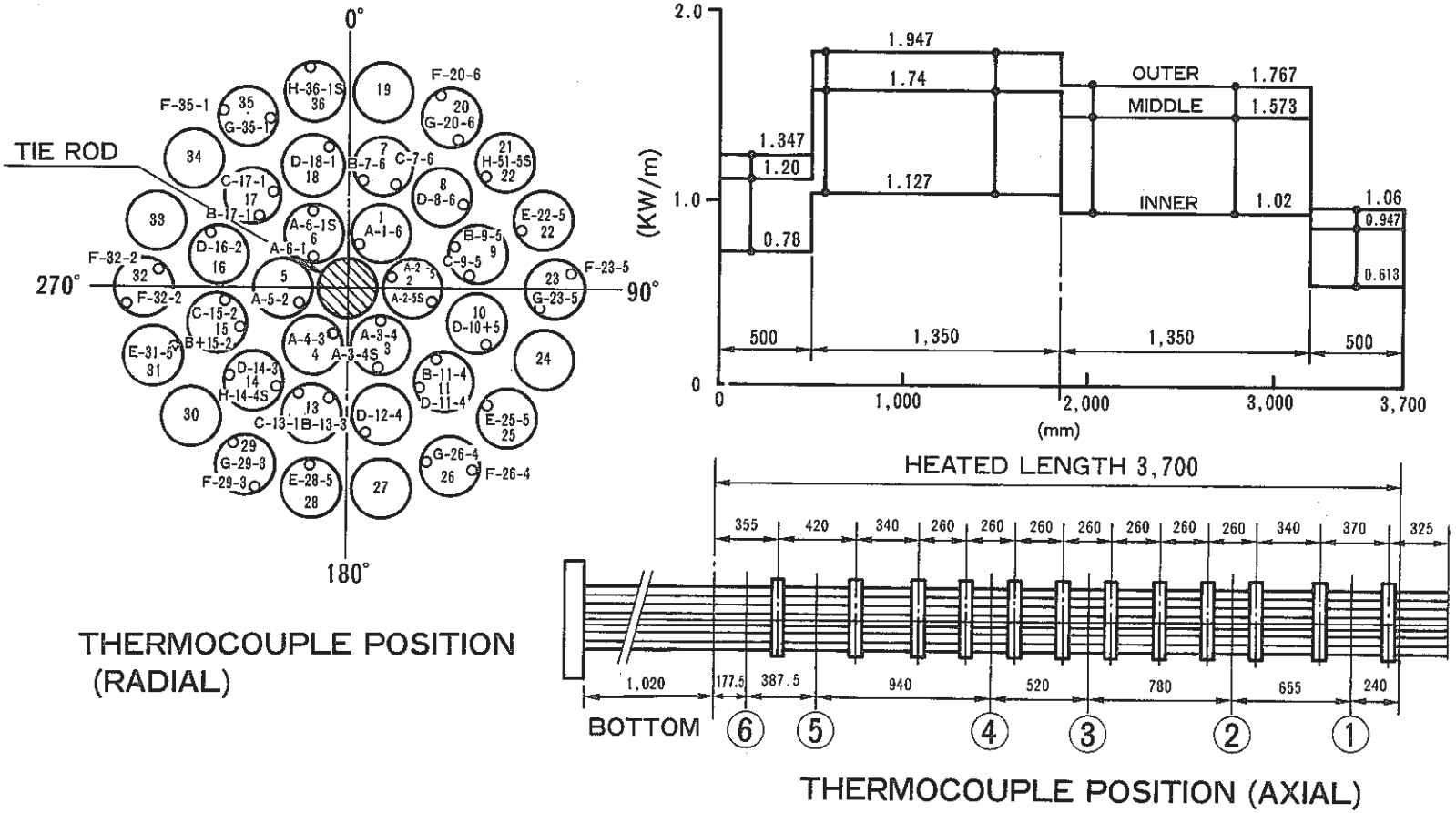

FIG. 3 POSITIONS OF THERMOCOUPLES

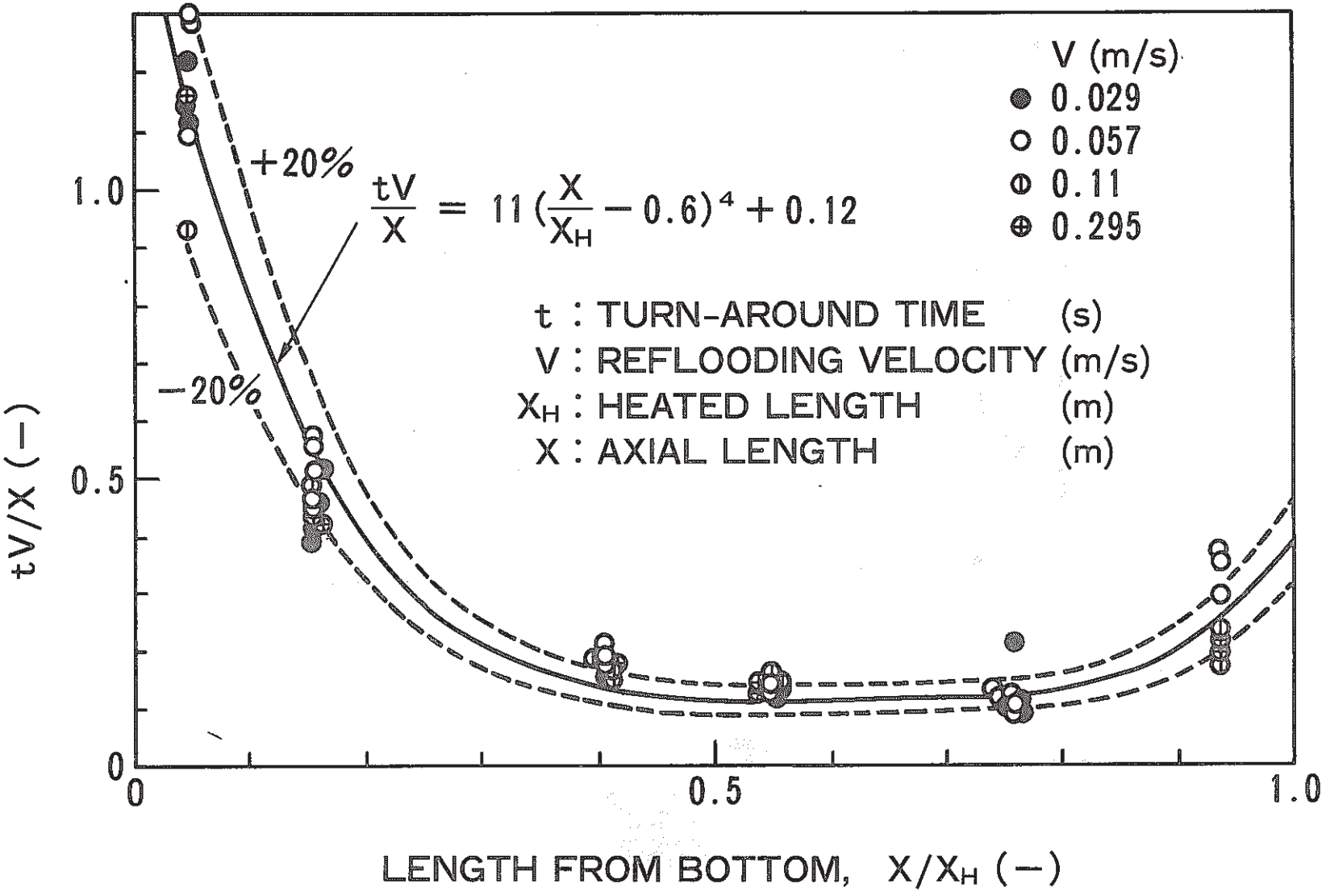

FIG. 4 NON-DIMENSIONAL TURN-AROUND TIME VS AXIAL LENGTH

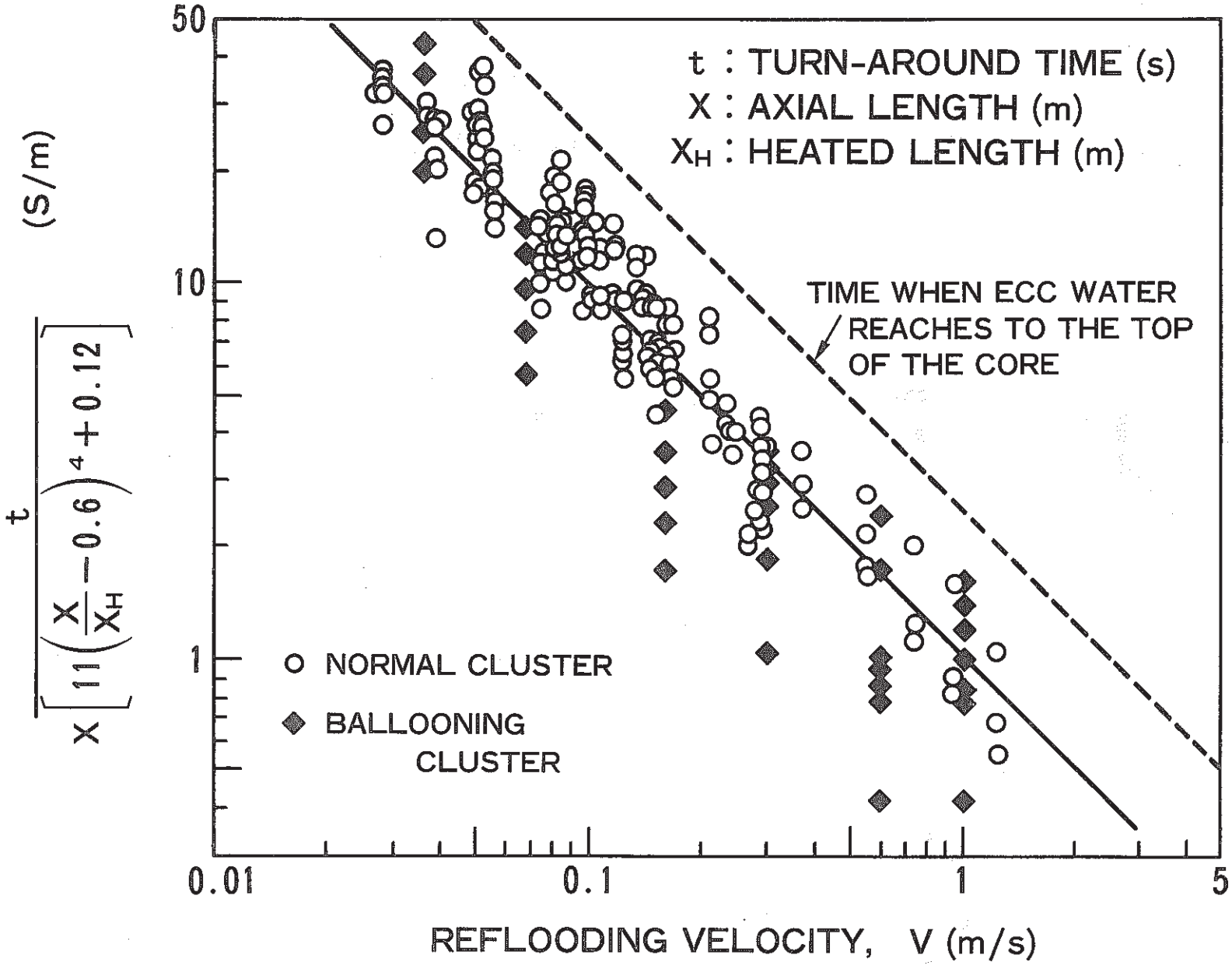

FIG. 5 RELATIONSHIP BETWEEN TURN-AROUND TIME AND REFLOODING VELOCITY

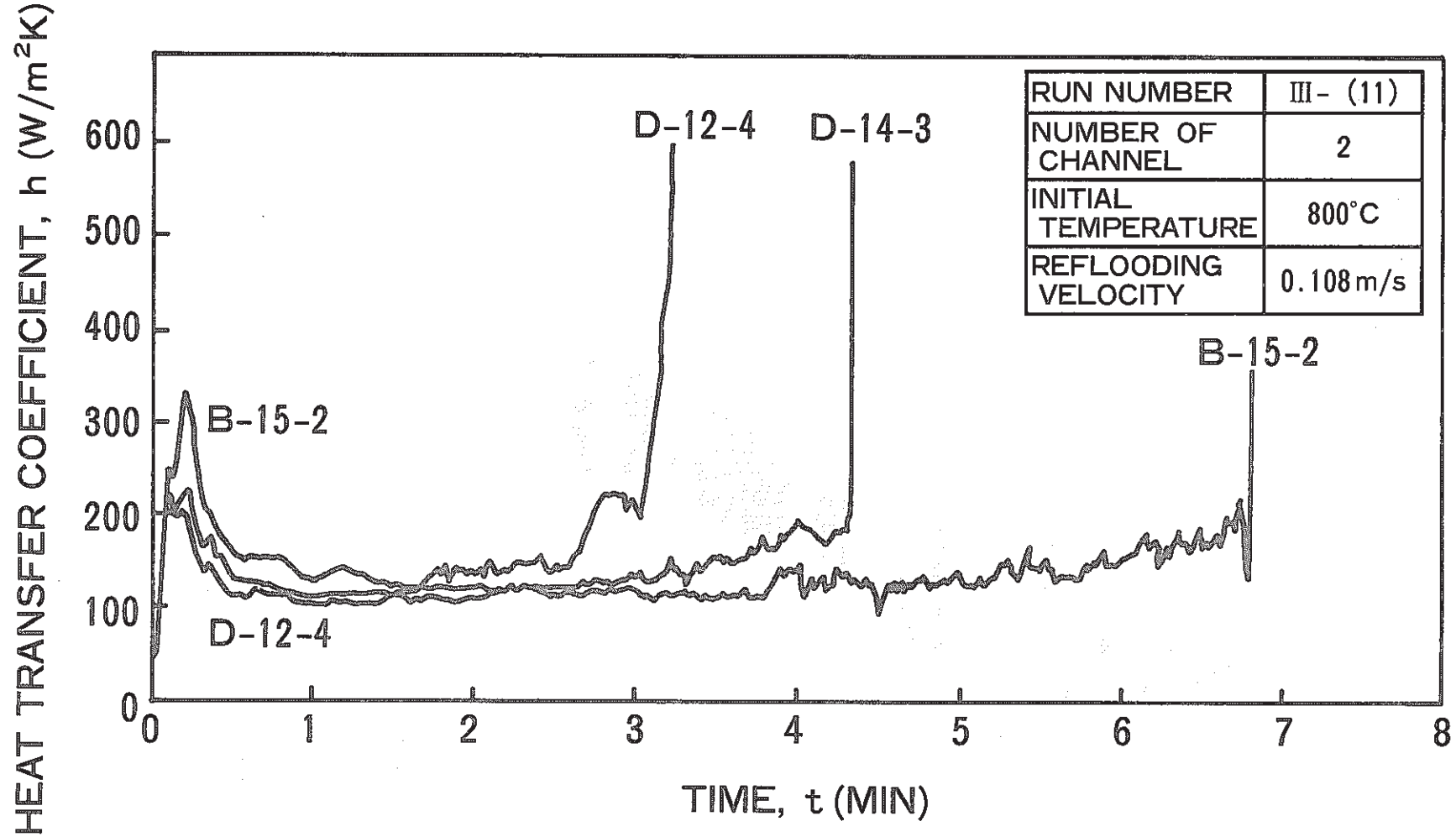

FIG. 6 TIME HISTORY OF HEAT TRANSFER COEFFICIENT AFTER TURN-AROUND

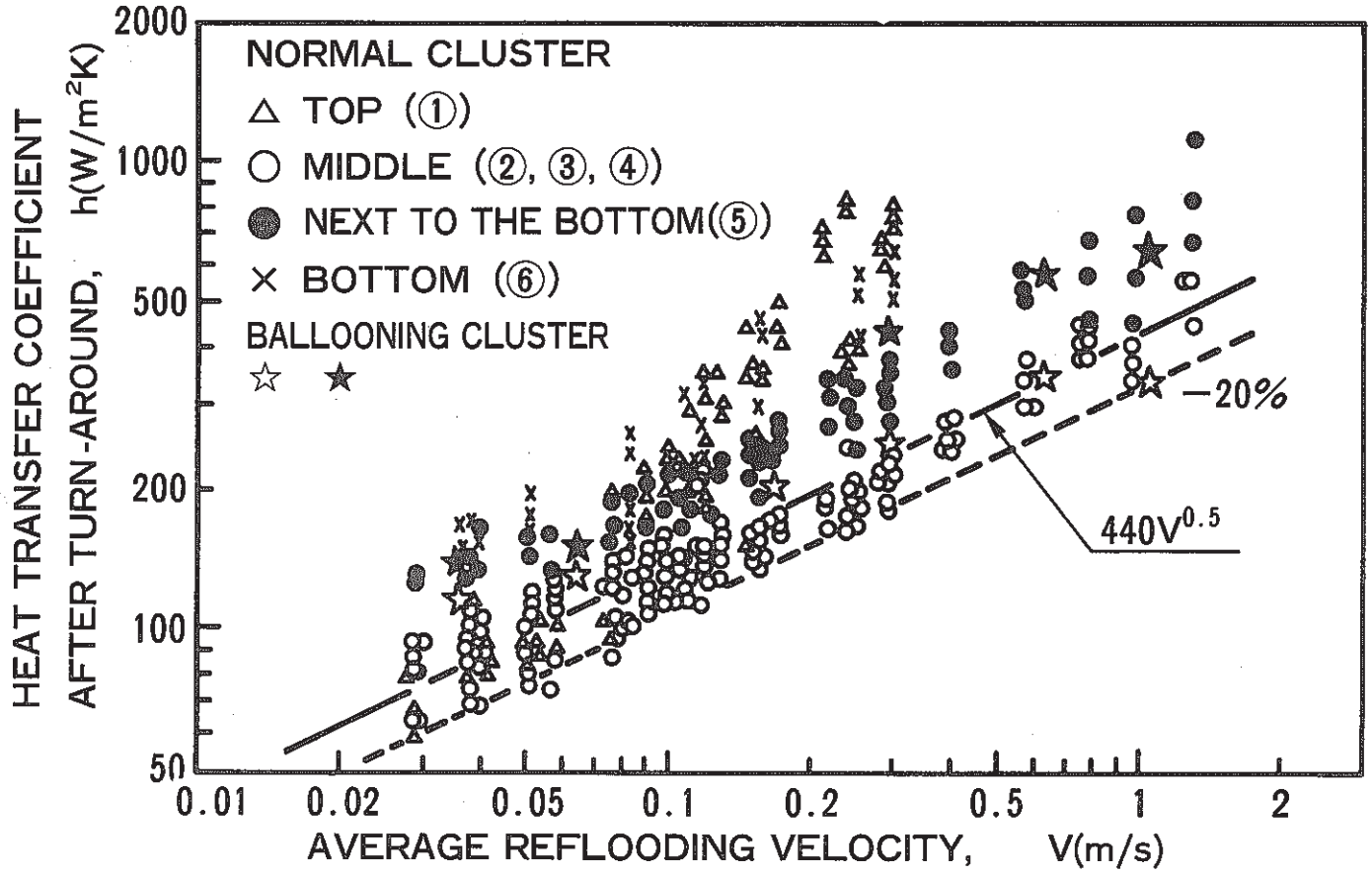

FIG. 7 HEAT TRANSFER COEFFICIENT AFTER TURN-AROUND

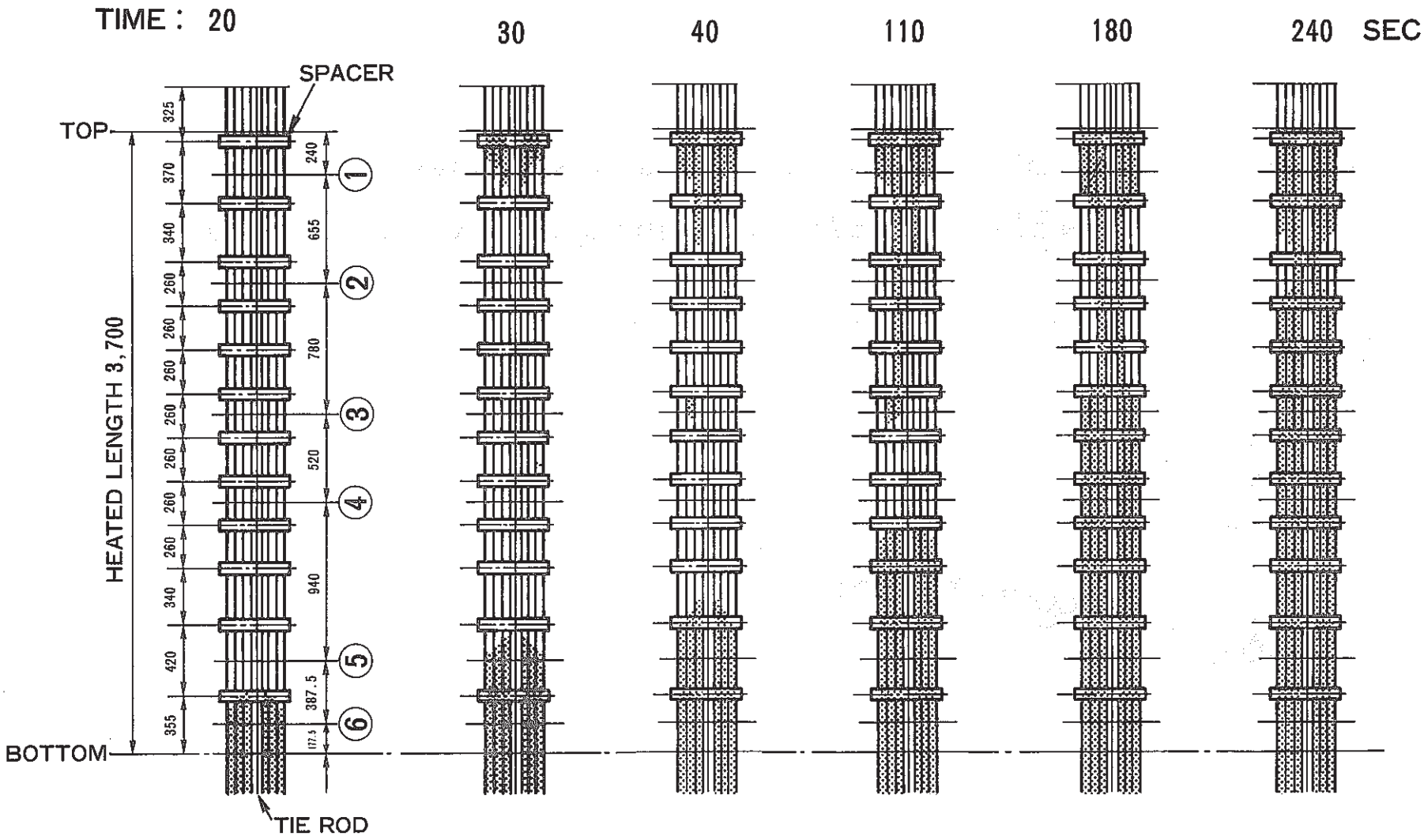

FIG. 8 QUENCHING BEHAVIOR FOR 36-ROD BUNDLE (V=0.156m/s)

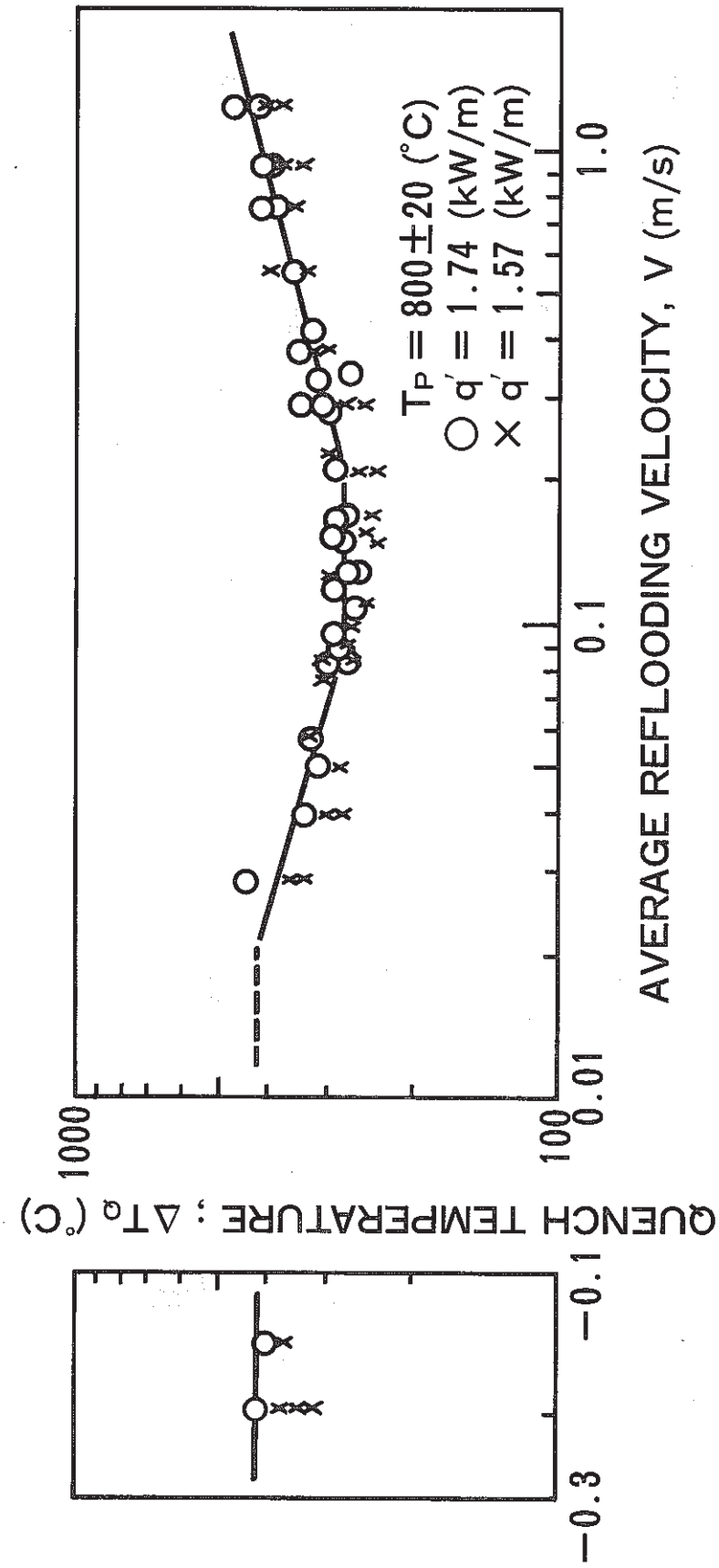

FIG. 9 RELATIONSHIP BETWEEN QUENCH TEMPERATURE AND AVERAGE REFLOODING VELOCITY

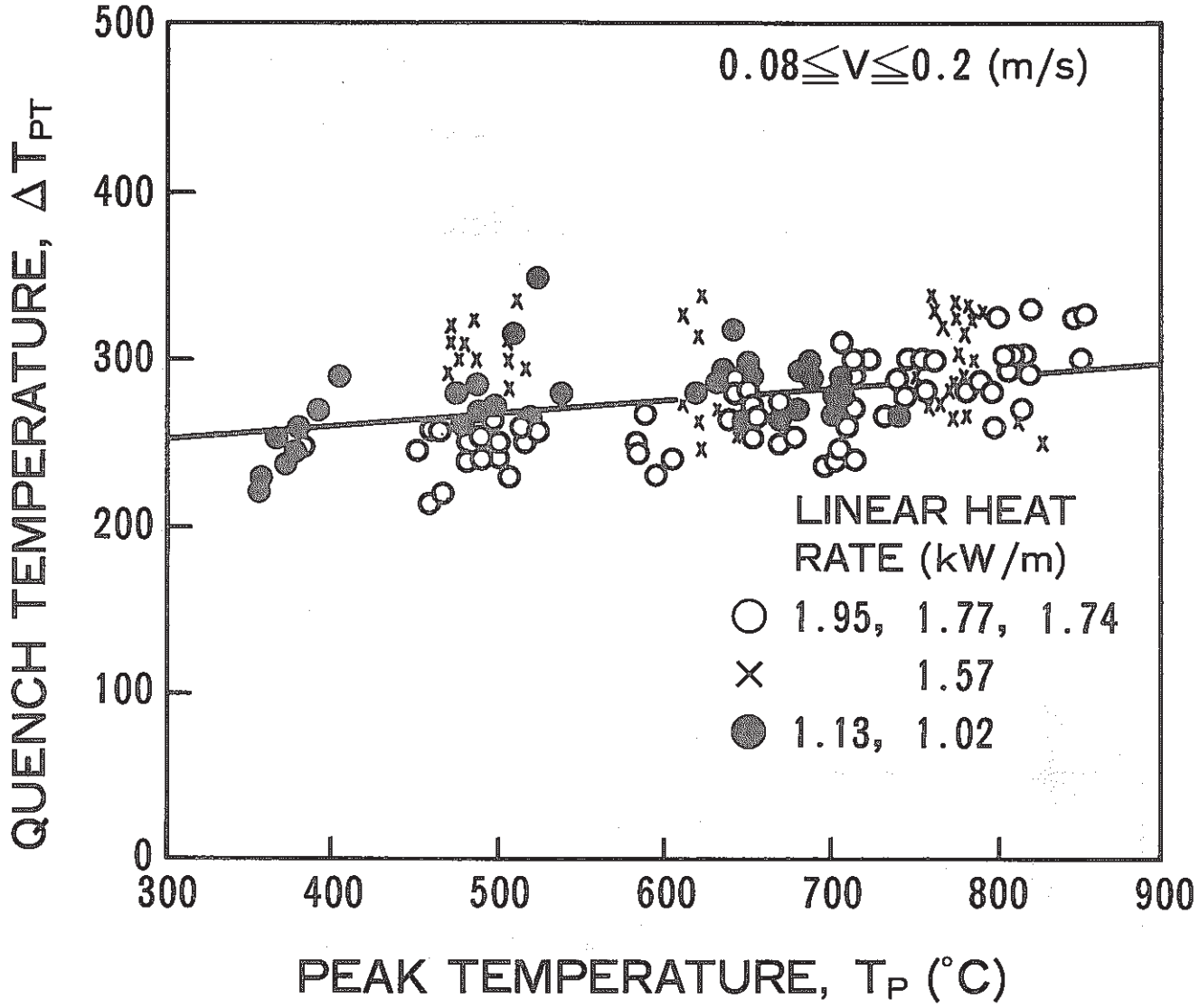

FIG. 10 RELATIONSHIP BETWEEN QUENCH TEMPERATURE AND PEAK TEMPERATURE

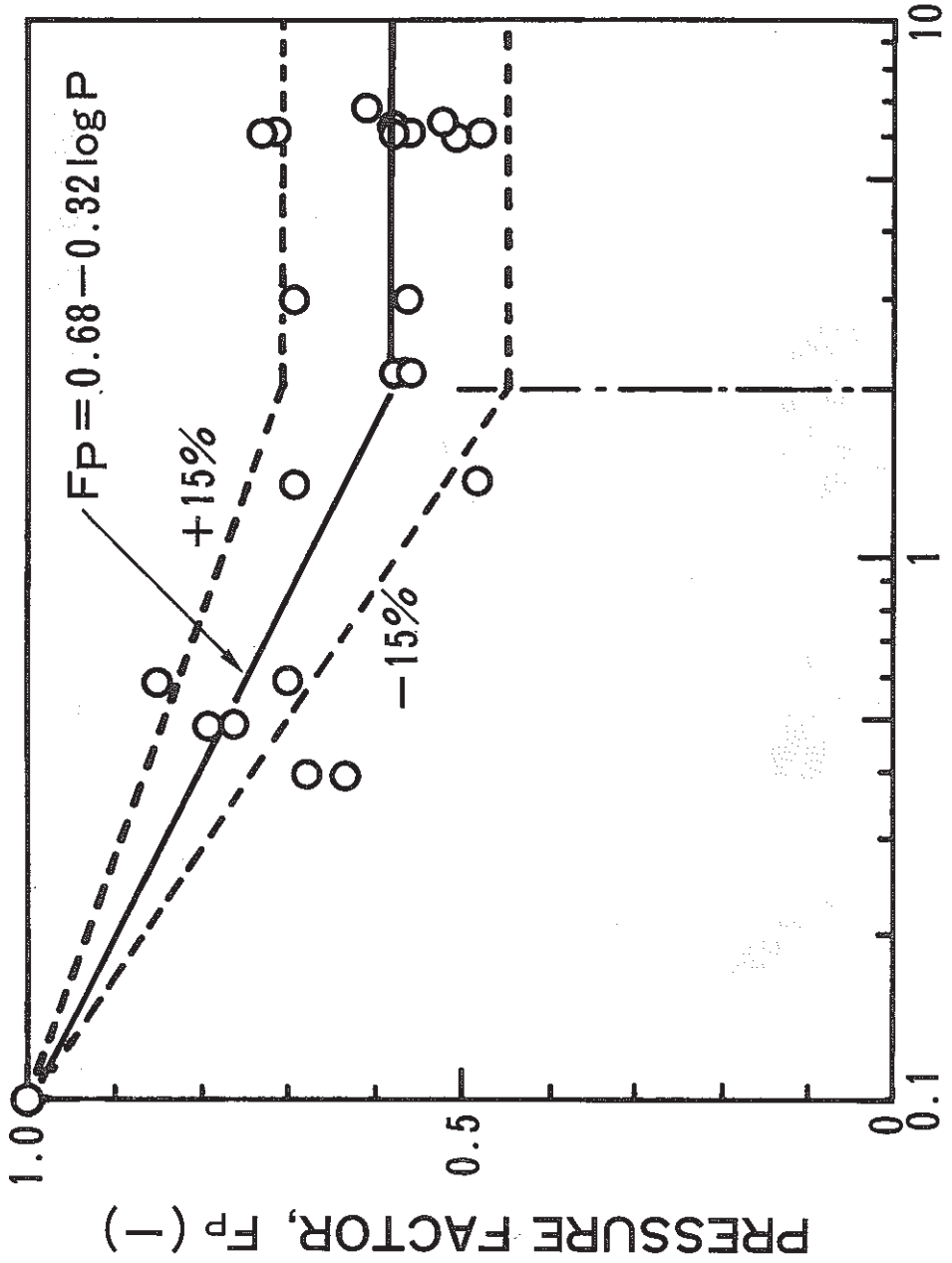

FIG. 11 EFFECT OF PRESSURE ON QUENCH TEMPERATURE

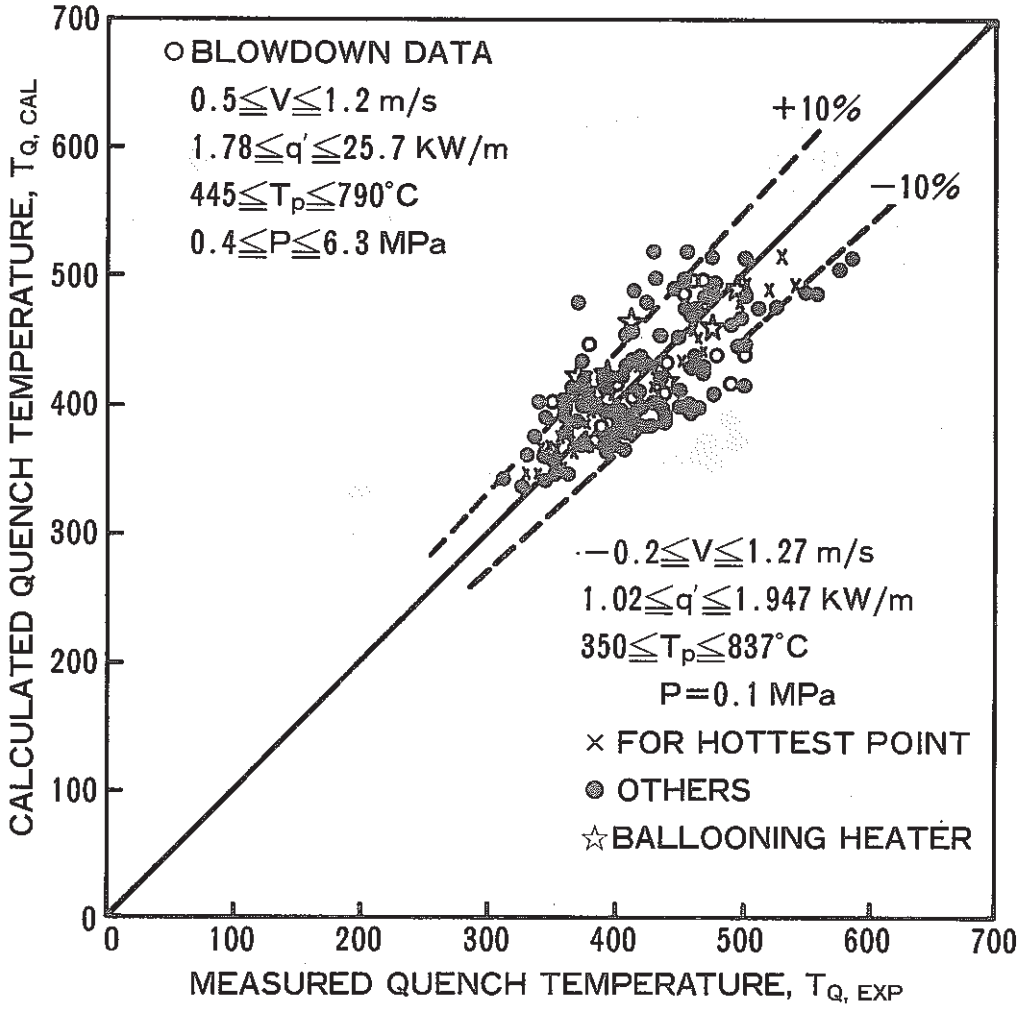

FIG. 12 COMPARISON OF QUENCH TEMPERATURE BETWEEN CALCULATED AND MEASURED

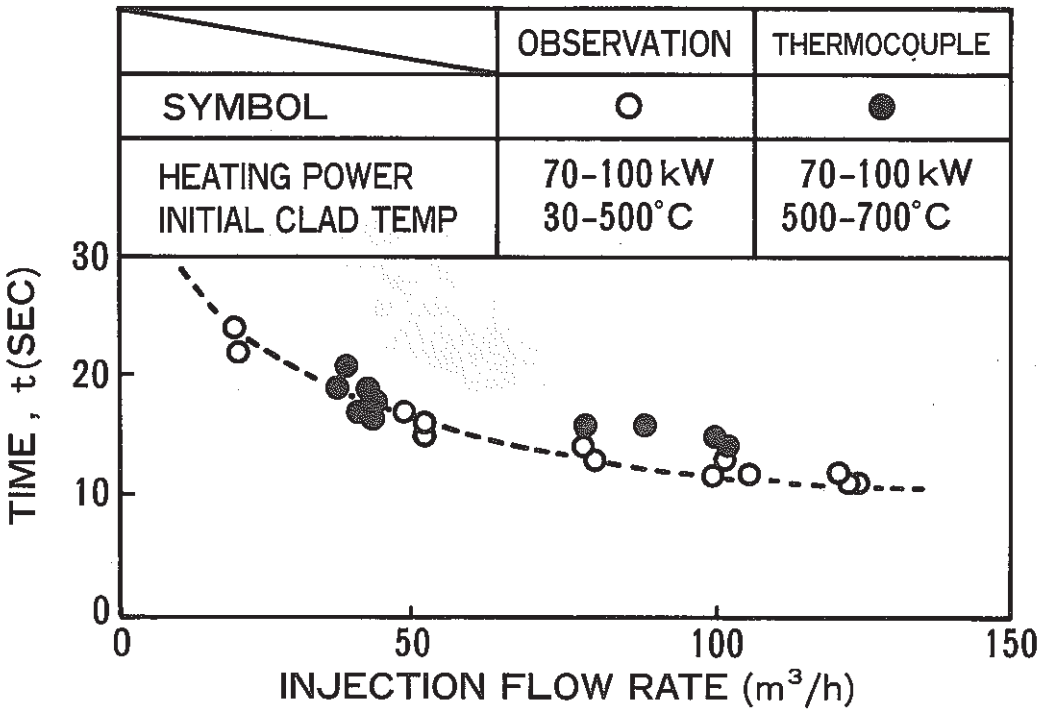

FIG. 13 EFFECT OF INJECTION FLOW RATE ON WATER ARRIVAL TIME TO THE CORE

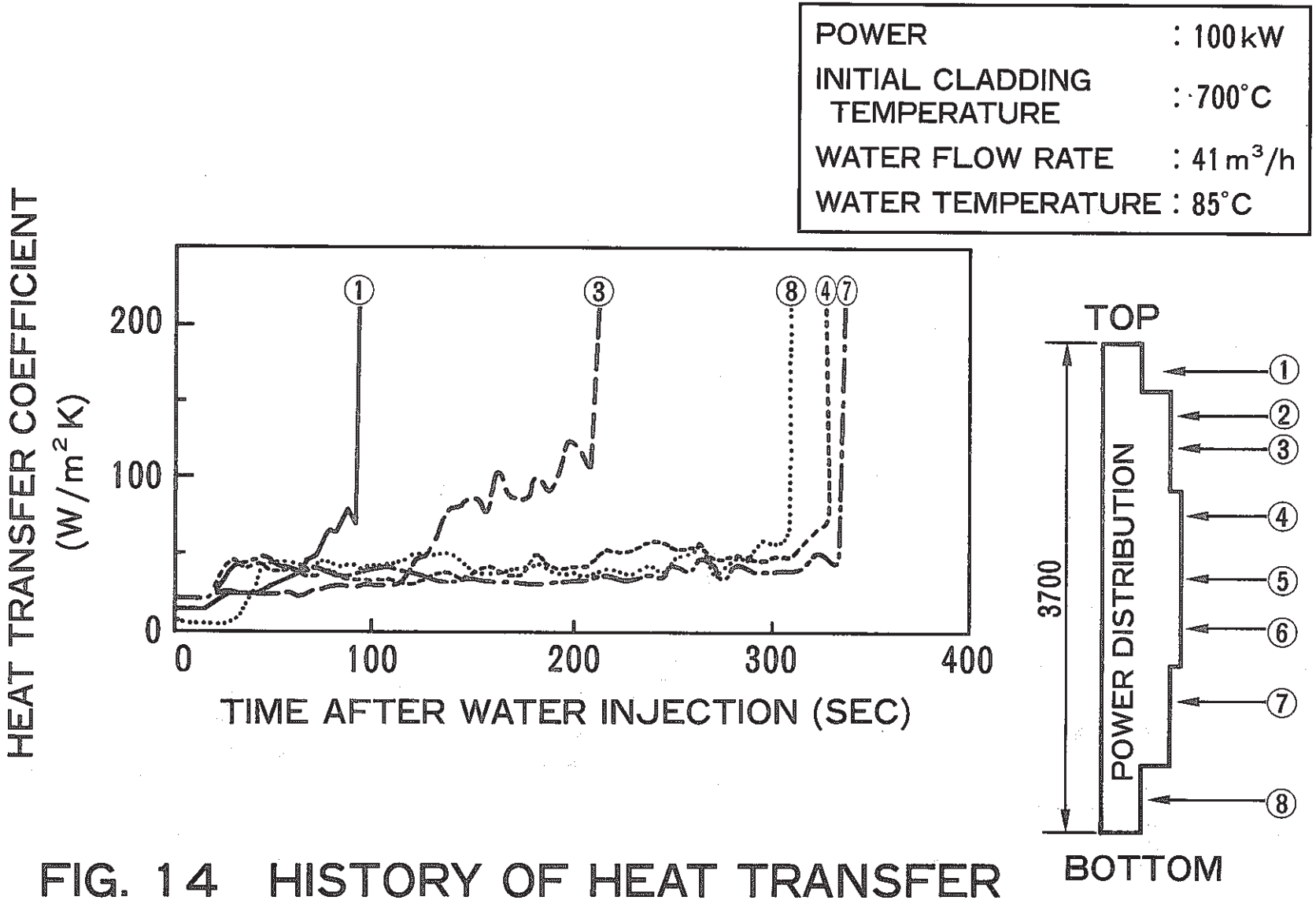

FIG. 14 HISTORY OF HEAT TRANSFER COEFFICIENT AFTER TOP FLOODING

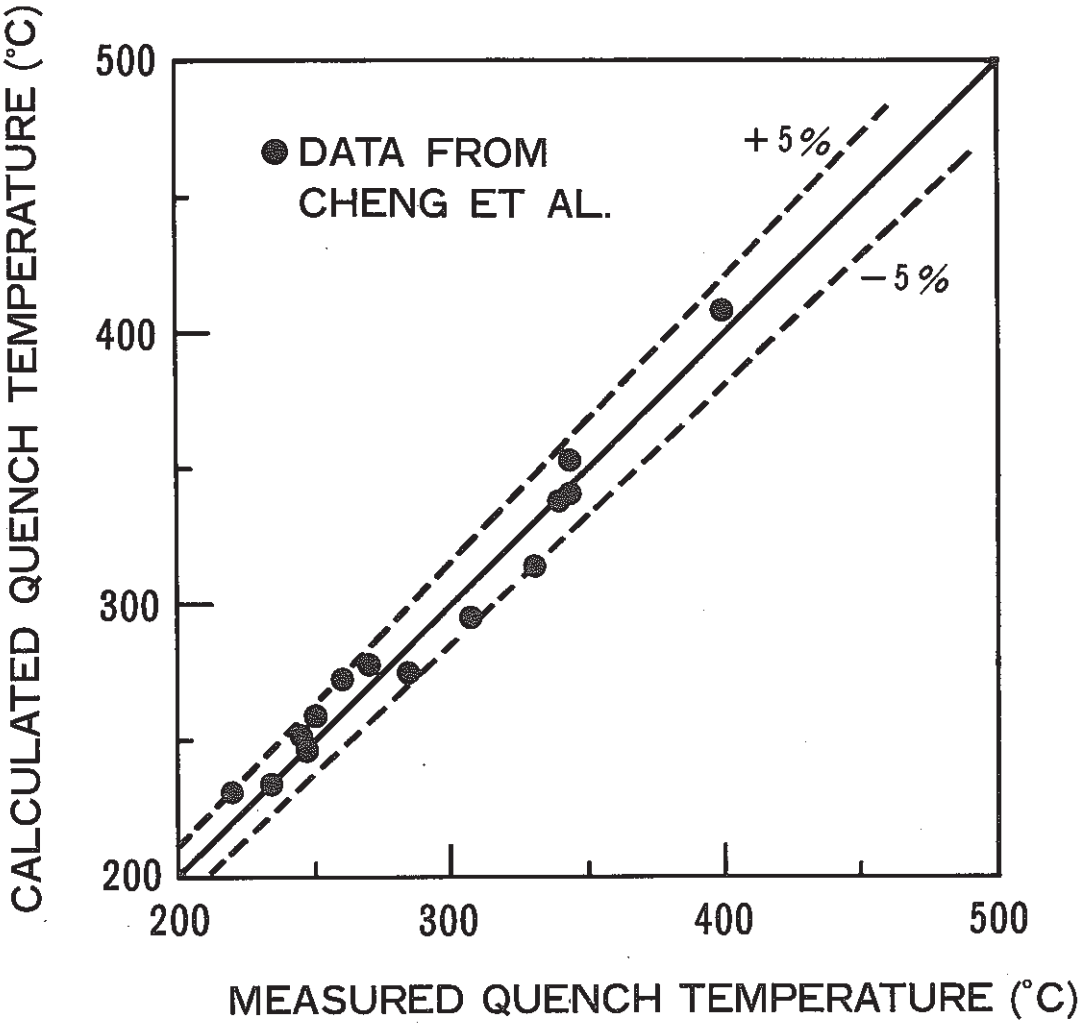

FIG. 15 COMPARISON OF QUENCH TEMPERATURE BETWEEN MEASUREMENT AND CALCULATION

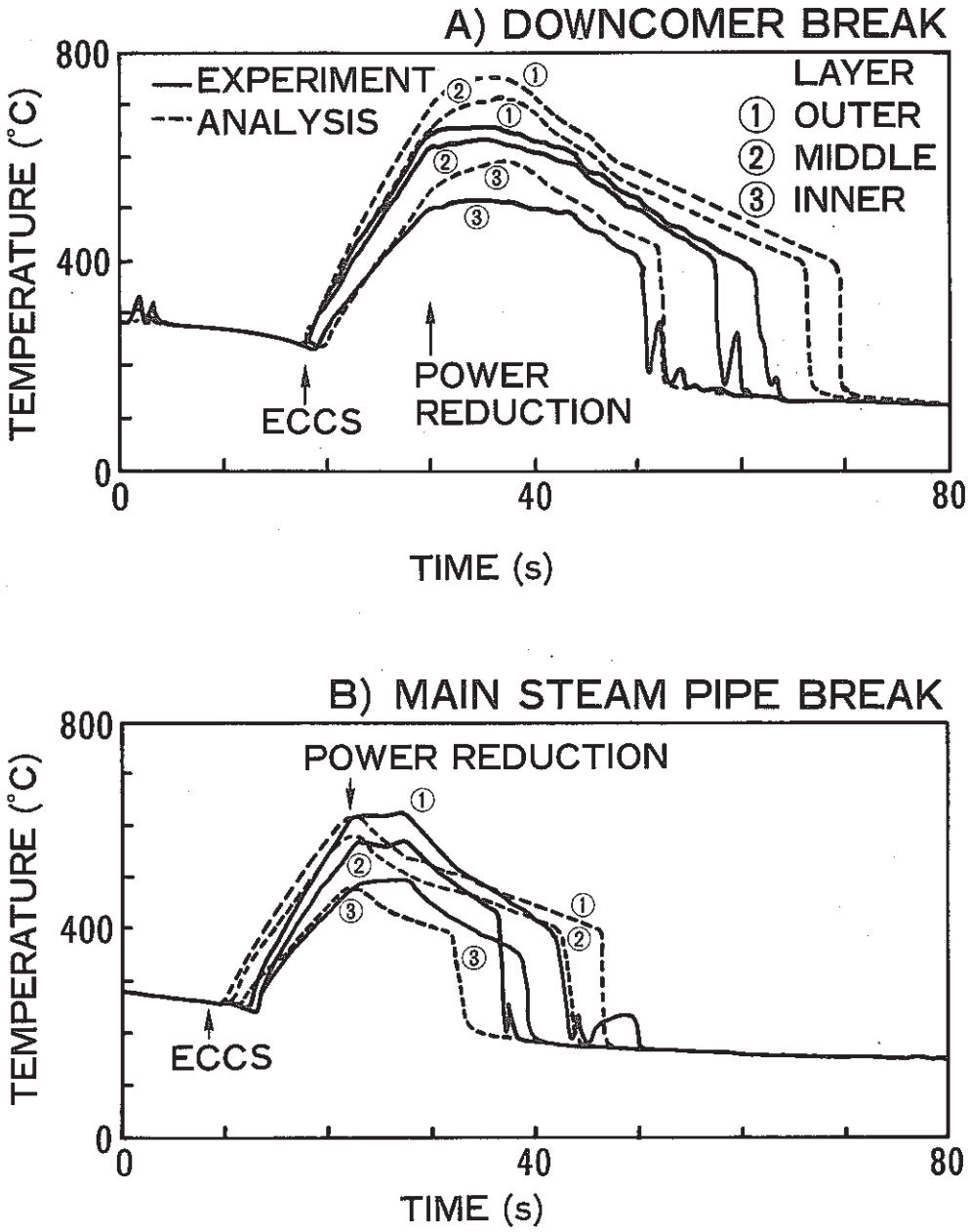

FIG. 16 BEHAVIORS OF CLADDING TEMPERATURES ASSOCIATED WITH 150 mm DOWNCOMER BREAK AND 150 mm MAIN STEAM PIPE BREAK